Active Disturbance Rejection Control of Unmanned Tracked Vehicle

Goran Banjac [1]
Momir Stanković[1]
Stojadin Manojlović[1]

Significant improvement of the unmanned vehicles possibility has achieved by increasing its autonomy, i.e. by excluding the human operator from the guidance loop. In this paper is considered the autonomous control of the unmanned tracked vehicle (UTV) in the presence of the unknown caterpillar tracks slippage. The longitudinal and lateral control model for the UTV path following problem are developed. To handle unknown uncertainties and slippage disturbances, the design of active disturbance rejection control (ADRC) for both, longitudinal and lateral control channels, are proposed. ADRC strategy is enabled that all the control channel uncertainties and disturbances are treated as one lumped (total) disturbance, which is defined as an extended system state and estimated by appropriate extended state observer (ESO). Further, applying the appropriate closed-loop control laws, based on the total disturbance estimation, the complex longitudinal and lateral control problems are reduced to disturbance-free model control. The numerical simulations for the different path following scenarios and caterpillar tracks slippage dynamics are given to verify effectiveness of the proposed UTV control.

Key words: Unmanned Tracked Vehicle, Active Disturbance Rejection Control, Extanded State Observer.

Introduction

IN recent years, autonomous unmanned vehicles have received significant attention. They are used for a wide variety of both civilian (transporting, assistance to disabled people, fumigation, harvesting, patrol monitoring and detection, investigation, exploration and inspection at tunnels, buildings, etc…) and military applications (as weapons platforms, logistics carriers, and surrogates for reconnaissance, surveillance, and target acquisition). Generally, the autonomous movement of vehicles requires integration of subsystems for navigations, guidance and control [1]. The navigation subsystem provides a data related to vehicle position in the space, using the different types of sensors (camera, radar, laser sensors, etc…) and/or global navigation system such (GPS, GLONASS, QZSS, Galileo, etc…). On the other hand, the guidance system provides the desired path of the vehicle, whose way of realization depending on the level of autonomy of the vehicle. It can be generated directly by a human (lowest level of autonomy) or by using self-governing sub-systems for path planning (higher levels of autonomy). However, regardless of the chosen navigation and guidance systems, from the control point of view, their outputs can be considered as feedback and reference signals for the control system. Then, control system by an appropriate control algorithm generates signals to vehicle driving actuators. The visual representation of overall autonomous vehicles system is shown in Fig.1.
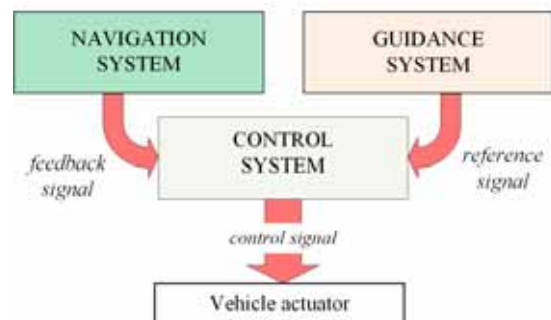

Figure 1. Structure of autonomous vehicles system

The aim of control algorithm is to ensure the robustness and stability of the movement, taking into account the dynamic behaviour and constructive limitations of the vehicle in presence of external disturbances, such as unknown slipping dynamics or the variable vehicle load. Therefore, the applications of the conventional control strategy, such as PI/PID structures, are usually limited [2, 3]. Among the many robust control approaches, active disturbance rejection control (ADRC) concept is standing out with a good trade-off between high control performances on the one side, and relative low complexity, on the other side. This algorithm has proven to be robust, effective and practical in suppressing both external and internal disturbances, such as vehicle unmodeled dynamics, system internal uncertainties and nonlinearities [3, 4, 5, 6]. It is enabled by the fact that ADRC algorithm treats all system uncertainties and disturbances as one total disturbance, which can be estimated by extended state observer (ESO) and then rejected in real-time using appropriate ADRC control law.

This paper proposes the application of ADRC-based control structure to enable complex path following of the unmanned tracking vehicle (UTV), in the presence of variable slippage dynamics. To handle unknown uncertainties and slippage disturbances, the design of ADRC, for both semi-coupled longitudinal and lateral control channels, are introduced. ADRC strategy is enabled that all the control channel uncertainties and disturbances are treated as one lumped (total) disturbance, which is defined as an extended system state. Total disturbance in both channels are estimated by appropriatly designed ESOs, and then rejected by ADRC control laws. The efficency of the proposed control strategy is tested through different simulation scenarious in complex path following problem in presence of the variable slippage dynamics.

UtV motion model

The motion model of the UTV can be described as:

$$
\begin{bmatrix} \dot{x}(t) \\ \dot{y}(t) \\ \dot{\theta}(t) \end{bmatrix} = \begin{bmatrix} \cos(\theta(t)) & 0 \\ \sin(\theta(t)) & 0 \\ 0 & 1 \end{bmatrix} \begin{bmatrix} v(t) + v_d(t) \\ \omega(t) + \omega_d(t) \end{bmatrix}, \quad (1)
$$

where coordinate $x(t)$ and $y(t)$ denotes vehicle position in the inertial coordinate system, $\theta(t)$ is angle orientation of UTV, $v(t)$ and $\omega(t)$ are longitudinal velocity and angular speed, respectively, both considered as the system control inputs. The uncertainties in the linear and angular velocity, caused by unknown track friction, i.e. track slippage, are represent with $v_d(t)$ and $\omega_d(t)$, respectively.

Including the dynamic model of UTV [5], the control inputs $v(t)$ and $\omega(t)$ can be defined as:

$$
v(t) = \frac{a}{2}(\omega_R(t) + \omega_L(t)), \quad (2)
$$

$$
\omega(t) = \frac{a}{2}(\omega_R(t) - \omega_L(t)), \quad (3)
$$

where *m* is the wheel radius, *b* is the normal distance between the right and left track, and (ω_R, ω_L) are the angular velocities of the right and left track wheel. In should be noted that ω_R and ω_L represents the control input of the real vehicle, both determined based on the designed control signals $v(t)$ and $\omega(t)$.

In the presence of the track slippage, (2) and (3) should be modified as:

$$
v(t) + v_d(t) = \frac{m}{2}(a_R \omega_R(t) + a_L \omega_L(t)), \quad (4)
$$

$$
\omega(t) + \omega_d(t) = \frac{m}{b}(a_R \omega_R(t) - a_L \omega_L(t)), \quad (5)
$$

where (a_R, a_L) are unknown friction coefficients of the right and left track, which are in the range [0,1].

From the previous analyses, one can see that UTV motion control involves design of subsystems for longitudinal velocity control (longitudinal controller) and for angular speed control (lateral controller).

Longitiudinal control design

To govern vehicle velocity in the presence of the slippage $v_v(t) = v(t) + v_d(t)$, longitudinal model of the UTV is formulated as:

$$
\dot{v}_v(t) = a(t) + \dot{v}_d(t), \quad (6)
$$

where $a(t) = \dot{v}(t)$ is control signal, which should be design to enable that $v_v(t)$ track the desired velocity $v_r(t)$ in the presence of the disturbance $v_d(t)$.

Applying ADRC concept for the first order system, the (6) can be represent in the state-space form as:

$$
\begin{bmatrix} \dot{v}_v(t) \\ \dot{f}_v(t) \end{bmatrix} = \begin{bmatrix} 0 & 1 \\ 0 & 0 \end{bmatrix} \begin{bmatrix} v_v(t) \\ f_v(t) \end{bmatrix} + \begin{bmatrix} 1 \\ 0 \end{bmatrix} a(t) + \begin{bmatrix} 0 \\ 1 \end{bmatrix} \dot{f}_v(t), \quad (7)
$$

where $f_v(t) = \dot{v}_d(t)$ represents the unknown the longitudinal channel total disturbance, which can be estimated by appropriate extended state observer:

$$
\begin{bmatrix} \dot{\hat{v}}_v(t) \\ \dot{\hat{f}}_v(t) \end{bmatrix} = \begin{bmatrix} 0 & 1 \\ 0 & 0 \end{bmatrix} \begin{bmatrix} \hat{v}_v(t) \\ \hat{f}_v(t) \end{bmatrix} + \begin{bmatrix} 1 \\ 0 \end{bmatrix} a(t) + \begin{bmatrix} l_1 \\ l_2 \end{bmatrix} e_v(t), \quad (8)
$$

where $e_v(t) = v_v(t) - \hat{v}_v(t)$ is observer error and l_1, l_2 are observer gains.

Active rejection of the total disturbance $f_v(t)$ can be realized by its estimation $\hat{f}_v(t)$ applying control law:

$$
a(t) = \dot{v}_r(t) + k_p(v_r(t) - v_v(t)) - \hat{f}_v(t), \quad (9)
$$

where k_p is adjustable controller parameter.

Assuming $\hat{f}_v(t) \approx f_v(t)$ and substituting (9) into (6) follows:

$$
\dot{v}_v(t) + k_p v_v(t) \approx \dot{v}_r(t) + k_p v_r(t), \quad (10)
$$

where one can see that desired control performances could be adjust by the appropriate selecting parameter k_p.

Lateral control design

To define lateral control model, consider the UTV path following problem shown in Fig.2, where the desired path is defined by moving of the virtual target:

$$
\begin{aligned} \dot{x}_r(t) &= v_r \cos(\theta_r) \\ \dot{y}_r(t) &= v_r \sin(\theta_r) \end{aligned}, \quad (11)
$$

where (x_r, y_r) are coordinates of the virtual target, v_r is the virtual target velocity (i.e. reference velocity of the vehicle) and θ_r is angle orientation of the virtual target in inertial coordinate system. Path following error vector $e(t)$ is defined in path-bound coordinate system by two components: lateral error $e_d(t)$ and along-track error $e_s(t)$, obtained as [2]:

$$
e(t) = \begin{bmatrix} e_s(t) \\ e_d(t) \end{bmatrix} = \begin{bmatrix} \cos(\theta_r) & \sin(\theta_r) \\ -\sin(\theta_r) & \cos(\theta_r) \end{bmatrix} \begin{bmatrix} x(t) - x_r(t) \\ y(t) - y_t(t) \end{bmatrix}, \quad (12)
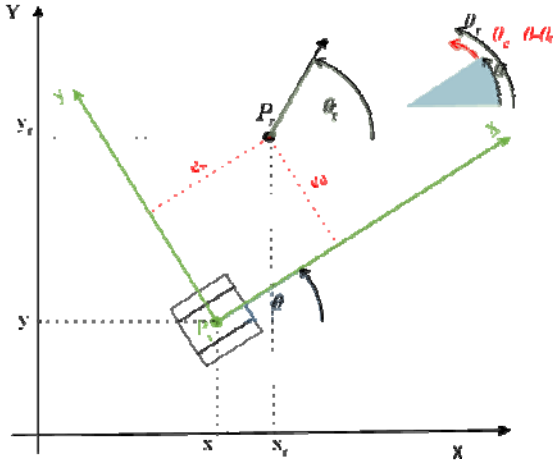$$

Figure 2. UTV path following problem

Denoting the course error angle as $\theta_e(t) = \theta(t) - \theta_r(t)$ and differentiating (7) follows:

$$\dot{e}_s(t) = \dot{\theta}_r(t)e_d(t) + v_r(t) + \big(v(t) + v_d(t)\big)\cos(\theta_e(t)),$$
$$\dot{e}_d(t) = \big(v(t) + v_d(t)\big)\sin(\theta_e(t)) + \dot{\theta}_r(t)e_s(t), \qquad (13)$$
$$\dot{\theta}_e(t) = \omega(t) + \omega_d(t) - \dot{\theta}_r(t)$$

As in practice the lateral error is main concern [4], lateral subsystem control can be formulated as a regulation control of the $e_d(t)$. Actually, the aim of the lateral subsystem control is to minimize $e_d(t)$ by the control input $\omega(t)$ in the presence of disturbances $v_d(t)$ iand $\omega_d(t)$. Therefore, the lateral model can be reformulated in the form:

$$\dot{e}_d(t) = v(t)\sin(\theta_e(t)) + d_1(t),$$
$$\dot{\theta}_e(t) = \omega(t) + d_2(t), \qquad (14)$$

where

$$d_1(t) = v_d(t)\sin(\theta_e(t)) + \dot{\theta}_r(t)e_s(t) \text{ and } d_2(t) = \omega_d(t) + \dot{\theta}_r(t)$$

are system disturbances. It sholud be noted that $d_1(t)$ represents mismatched uncertainty because it does not affect on the same input as control signal $\omega(t)$.

By differentiating and substituting, the model (14) can be presented in the more compact ADRC form as:

$$\ddot{e}_d(t) = v(t)\cos(\theta_e(t))\omega(t) + f_d, \qquad (15)$$

where $f_d(t) = \dot{v}(t)\sin(\theta_e(t)) + v(t)d_2(t)\cos(\theta_e(t)) + d_1(t)$ is the "total disturbance" of the lateral subsystem control, which is in the matched channel with the control signal $\omega(t)$. Also, it is evident that, even without system disturbances ($d_1(t) = d_2(t) = 0$), (14) has nonlinear dynamic that considered control problem makes challenging.

In the same as in longitudinal controller structure, the system (15) can be represent in the ADRC-based state-space model as:

$$\begin{bmatrix} \dot{e}_d(t) \\ \ddot{e}_d(t) \\ \dot{f}_d(t) \end{bmatrix} = \begin{bmatrix} 0 & 1 & 0 \\ 0 & 0 & 1 \\ 0 & 0 & 0 \end{bmatrix}\begin{bmatrix} e_d(t) \\ \dot{e}_d(t) \\ f_d(t) \end{bmatrix} +$$
$$+ \begin{bmatrix} 0 \\ v(t)\cos(\theta_e(t)) \\ 0 \end{bmatrix}\omega(t) + \begin{bmatrix} 0 \\ 0 \\ 1 \end{bmatrix}\dot{f}_d(t), \qquad (16)$$

Total disturbance can be estimate by extended state observer:

$$\begin{bmatrix} \dot{\hat{e}}_d(t) \\ \ddot{\hat{e}}_d(t) \\ \dot{\hat{f}}_d(t) \end{bmatrix} = \begin{bmatrix} 0 & 1 & 0 \\ 0 & 0 & 1 \\ 0 & 0 & 0 \end{bmatrix}\begin{bmatrix} \hat{e}_d(t) \\ \dot{\hat{e}}_d(t) \\ \hat{f}_d(t) \end{bmatrix} +$$
$$+ \begin{bmatrix} 0 \\ v(t)\cos(\theta_e(t)) \\ 0 \end{bmatrix}\omega(t) + \begin{bmatrix} l_{d1} \\ l_{d2} \\ l_{d3} \end{bmatrix}e(t), \qquad (17)$$

where $e(t) = e_d(t) - \hat{e}_d(t)$ is observer error and l_{d1}, l_{d2} and l_{d3} are observer gains. Utilizing a controller with disturbance rejection and estimated variables

$$\omega(t) = \frac{-k_{pl}\hat{e}_d(t) - k_{dl}\cdot\dot{\hat{e}}_d(t) - \hat{f}_d(t)}{v(t)\cdot\cos\theta_e(t)}, \qquad (18)$$

where k_{pl} and k_{dl} are adjustable controller parameters.

Assuming $\hat{f}_d(t) \approx f_d(t)$, $\hat{e}_d(t) = e_d(t)$, $\dot{\hat{e}}_d(t) = \dot{e}_d(t)$ and substituting (18) into (15) follows:

$$\ddot{e}_d(t) + k_{dl}\dot{e}_d(t) + k_{pl}e_d(t) \approx 0, \qquad (19)$$

where one can see that desired control performances could be adjust by the appropriate selecting parameters k_{pl} and k_{dl}. As a result, creating a control signal that assures the error accurately follows the provided dynamics (19) is the problem of following a certain path.

It should be noted longitudinal channel output $v(t)$ affects the UTV lateral control, but not vice versa. Therefore, the motion control of the UTV should be considered as the control problem of two semi-couple subsystems. Consequently, the architecture of the proposed two channel based UTV control is shown in Fig.3.
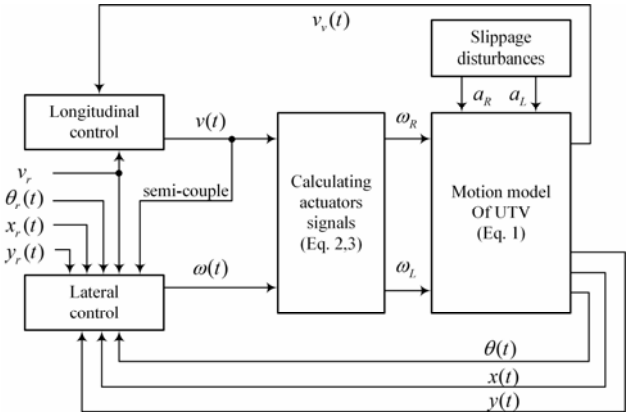

Figure 3. Control architecture of UTV

Simulation results

To verify the effectiveness of the proposed control algorithms the numerical simulations are performed based on considered UTV model with parameters $m = 0.1$m and $b = 1.4$m in presence of track slipping dynamics as $a_R = 0.15\sin(5t) + 0.65$ and $a_L = 0.85$. Two different simulations scenarios are assumed and that is presented in the following.

A. Simulation scenario 1: The straight-line reference trajectory tracking

In this scenario the given path represents straight line with

$\theta_r = \pi / 4$ and $v_r = 1 \, \mathrm{m/s}$. It is assumed that initial UTV coordinates are $x(0) = 0$, $y(0) = 0$ and $\theta(0) = 0$. The longitudinal controller coefficients are tuned based on pole placement method [7] as $\omega_{cv} = k_p$, and $l_1 = 2\omega_{ov}$, $l_2 = \omega_{ov}^2$, where $\omega_{cv} = 3 \, \mathrm{rad/s}$ and $\omega_{ov} = 9 \, \mathrm{rad/s}$ are longitudinal closed-loop system and observer bandwidth, respectively. Similarly the lateral controller coefficients are tuned as $k_{pl} = \omega_{cl}^2$, $k_{dl} = 2\omega_{cl}$, $l_{1l} = 3\omega_{ol}$, $l_{2l} = 3\omega_{ol}^2$, $l_{3l} = \omega_{ol}^3$, where $\omega_{cl} = 9 \, \mathrm{rad/s}$ is lateral closed-loop system bandwidth and the observer bandwidth is change through three cases:

$$C1: \omega_{ol} = 3\omega_{cl},$$
$$C2: \omega_{ol} = 6\omega_{cl},$$
$$C3: \omega_{ol} = 9\omega_{cl}.$$

The tracking results and the cross-track errors for all three cases are presented in Figures 4 and 5. From Fig.4 one can see that the tracking performance is highly consistent with the reference path, despite the presence of the track slippage. The high accuracy in following the reference path can also be seen by the cross-track error in Fig.5, but it is evident that system with the larger value of ω_{0l} achieves the better tracking performance in both transient steady-state (see zooming part of Fig.5).
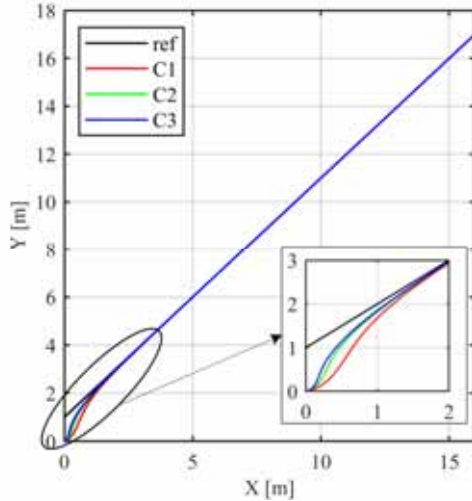

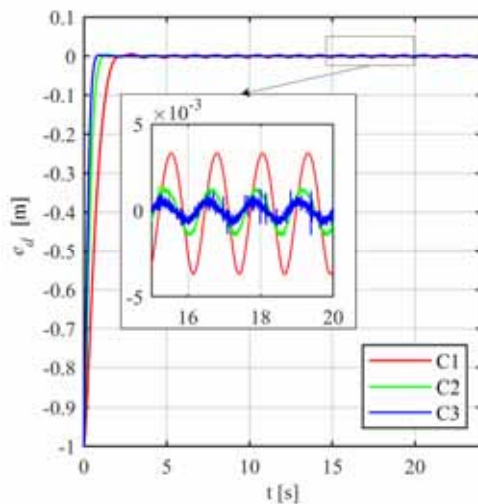**Figure 4.** Tracking results of the UTV

Figure 5. Cross-track errors of the AGV

The total disturbance estimation error $f_{ed}(t) = f_d - \hat{f}_d$ in lateral channel in steady state is gathered in Fig.6. It can be observed that all cases of ESO tuning provide reliable estimations performances which conduce to the strong capability of disturbance rejection. As it is expected, the better estimation quality and consequently the better tracking performance enables case C3. However, it is paid by larger value of the actuators control signals in transient depicted in left side of Fig.6, while the control signals for C2 and C1 are significantly lower in the transient and smoother in the steady state (right side of Fig.7).
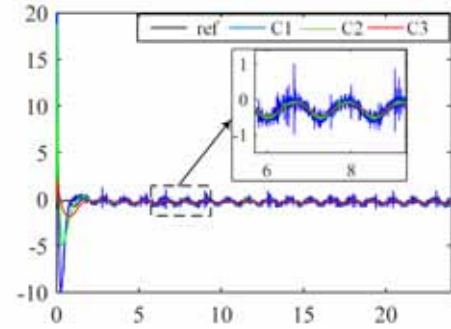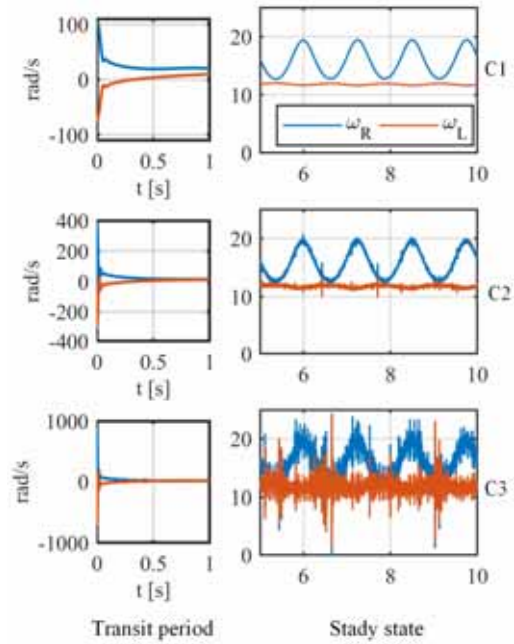

Figure 6. The total disturbance estimation error

Figure 7. Actuator control signals for cases C1, C2 and C3 in transient (left) and steady state (right)

B. Simulation scenario 2: The complex reference trajectory tracking

It this simulation scenarios the complex octagon path tracking is analyzed. Lateral closed-loop system and observer bandwidth are chosen as follows, , $\omega_{cl} = 3 \, \mathrm{rad/s}$, $\omega_{0l} = 9 \, \mathrm{rad/s}$, and for the longitudinal controller closed-loop system bandwidth is set as $\omega_{cv} = 3 \, \mathrm{rad/s}$, while following three cases of the observer bandwidth of longitudinal are considered:

$$C1: \omega_{ov} = 3\omega_{cv},$$
$$C2: \omega_{ov} = 6\omega_{cv},$$
$$C3: \omega_{ov} = 9\omega_{cv}.$$

Additionally, a noise is introduced into the measurement of both output signals, for lateral controller (e_d) and for

longitudinal controller (v_v), after tenth seconds of simulation.

The obtained UTV octagon trajectory tracking and cross track errors are shown in Figures 8 and 9, where one can note that the proposed control approach provides satisfied tracking performance for the octagon path, regardless of the variable track slipping and noise in measured feedback signals. Similarly as in previous simulation scenario, it is evident that the case C3, with the larger value of observer bandwidth, provides the better tracking accuracy

The total disturbance estimation signal in the longitudinal channel is presented in Fig.10. It can be seen that the measurement noise has the larger influence on systems with larger value of ω_{ov} (case C3), due to large value of observer gains in that case.

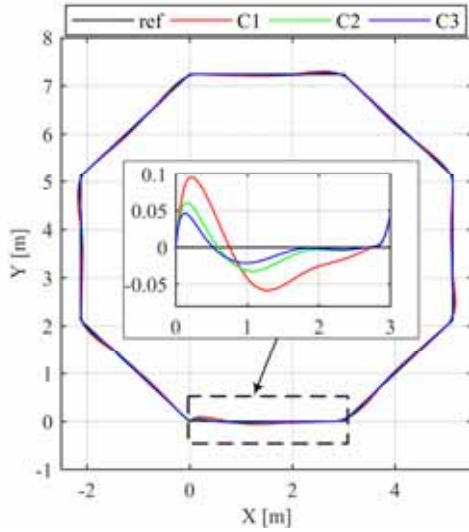**Figure 8.** The octagon reference trajectory tracking results for three cases of longitudinal controller observer bandwidth (C1, C2, C3)
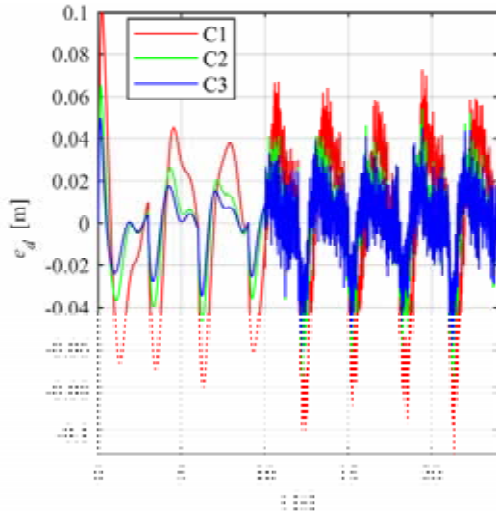

Figure 9. The octagon reference trajectory cross-track errors for three cases of longitudinal controller observer bandwidth (C1, C2, C3)

The results from Fig.11, shows the efficiency of the longitudinal controller, which enables satisfied control of the real vehicle speed v_v (hold it approximately equal to the speed of the reference point v_r =1m/s), by its output v in the presence disturbance v_d the reference. To avoid redundancy the results are presented only for case C3.

The actuator control signals are gathered in Fig.12, and it should be noted that these signals are similar. However, one can see that in the case C3 the signals reach the larger peak

values, which is the influence of the parameters varying and the measurement noise in the longitudinal channel.
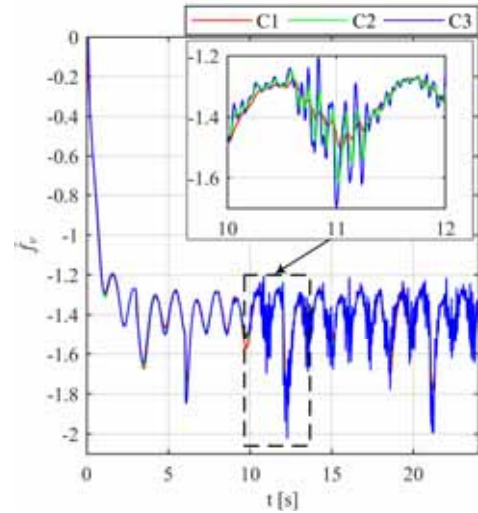

Figure 10. Longitudinal channel total disturbance estimation for three cases of longitudinal controller observer bandwidth (C1, C2, C3)
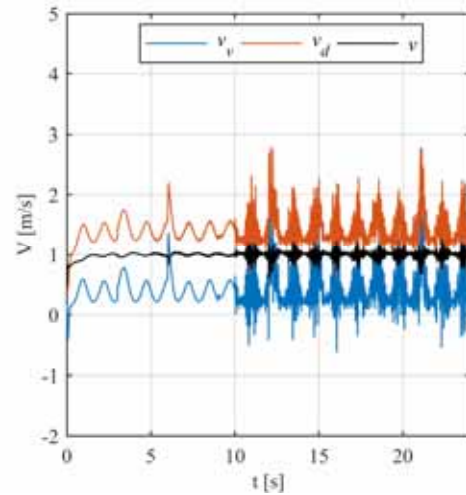

Figure 11. The real speed of the UTV (v_v), output of the longitudinal controller (v) and longitudinal disturbance (v_d) for C3 case of longitudinal controller setup

Conclusion

The new UTV control strategy based on ADRC longitudinal and lateral controllers are proposed. The appropriatly designed forms of ESOs and control laws are enabled estimation and rejection of the internal and external disturbances in the control channels and consequently high path following system performances. The proposed control structure is tested by Matlab/Simulink numerical simulations through two scenarios of path following problem in the presence of variable track slippage dynamics. The achieved results have validated the suggested UTV control solution, and the further work will be focused to implementation of the designed controllers to real UTV and experimental verifications.
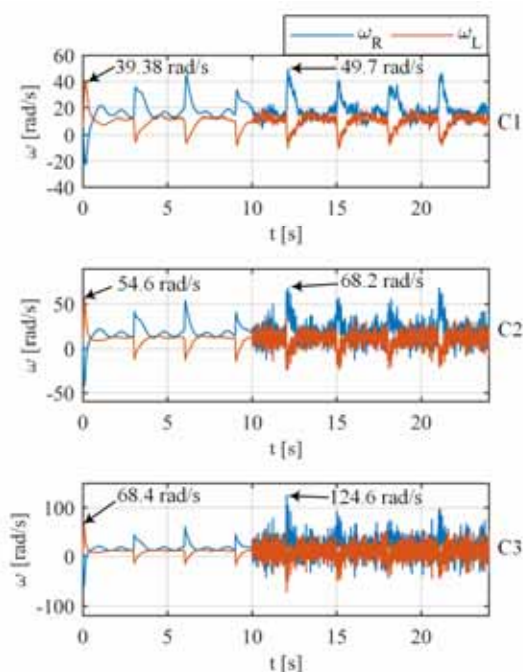
Acknowledgment

Figure 12. Actuator control signals for the case C1, C2 and C3

References

[1] NONAMI,K., KARTIDJO,M., YOON: A*utonomous Control Systems and Vehicles,* Intelligent Systems, Control and Automation: Science and Engineering*,* 2013.

[2] CHEN,S., WENCHAO,X., ZHIYUN,L., YI H.: *On Active Disturbance Rejection Control for Path Following of Automated Guided Vehicle with Uncertain Velocities,* American Control Conference (ACC) Philadelphia, pp.2446-2451, July, 2019.

[3] CHEBLY,A., TALJ,R.& CHARARA,A.: *Coupled longitudinal/lateral controllers for autonomous vehicles navigation, with experimental validation*, Control Engineering Practice, 88, 79–96., 2019

[4] CHEN,S., XUE,W., LIN,Z., HUANG,Y.: *On active disturbance rejection control for path following of automated guided vehicle with uncertain velocities*, In 2019 American Control Conference (ACC), pp. 2446-2451, IEEE, 2019.

[5] STANKOVIĆ,M., MANOJLOVIĆ,S.: *Autonomno kretanje besposadnog vozila po zadatoj putanji primenom algoritma sa aktivnim potiskivanjem poremećaja*, ETRAN, Republika Srpska, Stanišić, 2021.

[6] WANG,H., ZUO,Z.,WANG,Y., YANG,H., CHANG,S.: *Composite nonlinear extended state observer and its application to unmanned ground vehicles*, Control Engineering Practice 109, 2021.

[7] GAO Z: *Scaling and bandwidth-parameterization based controller tuning*, Proceedings of the 2003 American Control Conference, 2003.

Regulator sa aktivnim potiskivanjem poremećaja na besposadnim guseničnim vozilima

Značajno unapredjenje mogućnosti besposadnih vozila postignuto je povećanjem njihove autonomije, odnosno, isključivanjem ljudskog operatera iz petlje navođenje. U ovom radu se razmatra autonomno upravljanje besposadnim guseničnim vozilom (BGV) u prisustvu spoljašnjeg poremećaja u obliku proklizavanja pogonskih gusenica. Kako bi bio rešen problem praćenja referentne putanje projektovani su regulatori za longitudinalni i lateralni kanal upravljanja BGV-a. U cilju potiskivanja svih unutrašnjih i spoljašnih poremećaja, predložen je pristup baziran na regulatoru sa aktivnim potiskivanjem poremećaja (Active Disturbance Rejection Control - ADRC). Ovim pristupom je omogućeno da se svi navedeni poremećaji objedine u jedan totalni (ukupni) poremećaj, koji se definiše kao prošireno stanje sistema i procenjuje odgovarajućim opserverom proširenog stanja (Extended state Observer - ESO). Kako je pomoću ADRC ostvareno potiskivanje svih poremećaja u unutrašnjoj upravljačkoj petlji, spoljašna upravljačka petlja je rasterećena od njihovog uticaja, pa se celokupni problem upravljanja svodi na upravljanje modelom BGV-a bez smetnji. Verifikacija izabranog načina upravljanja je uradjena kroz numeričke simulacije za različite scenarije praćenja referentne putanje, uz uvodjenje spoljašneg poremećaja u obliku proklizavanja pogonskih gusenica

Ključne reči: besposadno gusenično vozilo, regulator sa aktivnim potiskivanjem poremećaja, opserver proširenog stanja.